JOURNAL OF SOLID STATE CHEMISTRY **131,** 78–83 (1997)
ARTICLE NO. SC977347

Synthesis, Characterization, and ^{1}H and ^{71}Ga MAS NMR Spectroscopy of a Novel Mg/Ga Double Layered Hydroxide

María Angeles Aramendía, Victor Borau, César Jiménez, José Maria Marinas, Francisco José Romero, and José Rafael Ruiz

Department of Organic Chemistry, Faculty of Sciences, Córdoba University, Av. San Alberto Magno s/n, E-14004 Córdoba, Spain

Received July 19, 1996; in revised form February 10, 1997; accepted February 14, 1997

A new brucite-like layered Mg/Ga double hydroxide (LDH) of composition $[Mg_{0.174}Ga_{0.256}(OH)_2](CO_3)_{0.134}\cdot mH_2O$ was synthesized by coprecipitation at pH 10. The hydroxide and the mixed oxides resulting from its thermal decomposition at 523, 823 and 1073 K were characterized by X-ray diffraction, diffuse reflectance infrared spectroscopy, high-resolution solid-state nuclear magnetic resonance (MAS NMR), and thermogravimetric analysis. The surface properties of the solid (specific surface) and its basicity were also determined. The Mg/Ga LDH was found to be stable up to 523 K and to decompose into a mixture of periclase MgO and amorphous Ga_2O_3 at 823 K. Its changes with temperature were monitored by using ^{1}H and ^{71}Ga MAS NMR; ^{1}H MAS NMR spectra revealed the loss of interlayer OH groups supporting the brucite-like structure on calcination at 823 K.
© 1997 Academic Press

INTRODUCTION

Layered double hydroxides (LDH) are of the general formula $[M(II)_{1-x}M(III)_x(OH)_2][A^{n-}]_{x/n}\cdot mH_2O$, where M is a metal and A an anion. These hydroxides can be used as precursors for multicomponent catalysts including the following:

(a) basic catalysts formed from Mg/Al LDHs and used in aldol condensation (1–3), alkylation (4), Claisen–Schmidt (5), and epoxide and lactone polymerization reactions (6, 7), among others;
(b) hydrogenation catalysts formed from Ni/Al, Zn/Cr, Cu/Zn/Al(Cr), and Cu/Co/Al(Cr) LDHs (8–12);
(c) steam reforming catalysts obtained from Ni/Al LDHs (12–14).

In addition, LDHs subjected to no thermal pretreatment following their synthesis are effective adsorbents (15, 16), chromatographic stationary phases (17), and ion exchangers (18).

The changes in LDHs during calcination are well documented (19, 20). Below 473 K, they only lose interstitial water; on the other hand, at 723–772 K, they undergo thorough dehydroxylation and decomposition of all carbonate into carbon dioxide and the corresponding metal oxide. In Mg/Al LDHs, the calcination residue obtained at the last temperature is of approximate composition $Mg_6Al_2O_8(OH)_2$. This product can be used to restore the LDH structure by rehydration in the liquid or vapor phase provided the calcination temperature is kept below 823–873 K. This is known as a "memory effect." Calcination at 723–773 K increases the surface area and pore volume of the solid slightly (19, 21) and results in a change in X-ray diffractograms from the LDH to a poorly crystalline magnesium oxide.

In one of the earliest items of research on the thermal decomposition of Mg/Al LDHs, Miyata *et al.* (21) characterized a number of anion sites in the product that had variable pK_b values. Therefore, M^{2+}/M^{3+} LDHs and the solids resulting from their calcination can be assumed to be basic in nature.

A wide variety of LDHs containing various di- and tervalent cations (Mg, Zn, Cr, Al, Fe, Ni, Co) and univalent cations (Li) in combination with different anions (CO_3^{2-}, SO_4^{2-}, NO_3^-, PO_4^{3-}, Cl^-, ClO_4^-) have been reported (22). Many of them are Mg/Al LDHs; few, however, contain Ga^{3+} (23). Although gallium belongs to the same group as aluminium (ionic radius = 0.50 Å), the former possesses a larger atomic volume (ionic radius = 0.62 Å), so its inclusion can distort LDH layers. In any case, the effects of introducing a bulkier, more basic cation than aluminium in an LDH on the structural and catalytic properties of the solid are theoretically quite interesting.

There are reported ^{71}Ga MAS NMR data that can help study LDHs containing this ion in crystallographic and physicochemical terms (24, 25). Gallium can replace aluminium in many crystal structures such as perovskites and zeolites. Most recently reported data in this respect were obtained by using high fields under MAS conditions and

0022-4596/97 $25.00
Copyright © 1997 by Academic Press
All rights of reproduction in any form reserved.

appropriate techniques for averaging the second-order quadrupole broadening involved.

The aim of this initial work on this type of solid was to synthesize a new Mg/Ga LDH and characterize it following various thermal treatments, by using different experimental techniques including diffuse reflectance infrared (DRIFT) spectroscopy, X-ray diffraction (XRD), and proton and gallium high resolution solid-state nuclear magnetic resonance (MAS NMR). The surface properties of the materials obtained from the different thermal treatments were also determined.

EXPERIMENTAL

Synthesis

The Mg/Ga LDH was obtained by using the coprecipitation method. For this purpose, two solutions containing 0.03 *M* $Mg(NO_3)_2 \cdot 6H_2O$ and 0.01 *M* $Ga(NO_3)_3 \cdot 6H_2O$, respectively, in 25 ml of deionized water $[x = Ga^{3+}/(Mg^{2+} + Ga^{3+}) = 0.25]$ were used. The mixture was slowly dropped over 75 ml of an Na_2CO_3 solution at pH 10 at 333 K, with vigorous stirring. The pH was kept constant by adding appropriate volumes of 1 *M* NaOH during precipitation. The suspension thus obtained was kept at 353 K for 24 h, after which the solid was filtered and washed with 2 liters of deionized water. The final solid was white-colored and named HT-1. Any residual nitrate ions in the LDH structure were removed by exchange with carbonate ions. For this purpose, 2.5 g of the LDH was dispersed in 125 ml of distilled water. The dispersion was supplied with 250 mg of Na_2CO_3 and refluxed for 2 h, after which the solid, white, was separated by centrifugation and the water discarded. This operation was repeated and supernatant analyzed for nitrate, which gave a negative test. The solid was then dried at 393 K and named HT-2. This solid was treated with nitrogen at a variable temperature for 8 h. The treatment at 523 K led to solid HT-3, whereas those at 823 and 1073 K gave solids HT-4 and HT-5, respectively.

Chemical Composition

The elemental composition of the sample was determined on a Perkin–Elmer 1000 ICP spectrophotometer under standard conditions.

X-Ray Diffraction

XRD patterns were recorded on a Siemens D 500 diffractometer using Cu$K\alpha$ radiation. Scans were performed over the 2θ range from 2 to 80.

Diffuse Reflectance Infrared Spectroscopy

DRIFT spectra for the solids were recorded from 400 to 4000 cm^{-1} on a Bomen MB-100 FTIR spectrophotometer. The sample was prepared by mixing 0.14 g of powdered solid with KBr (the blank) in a 15 : 85 ratio.

Thermal Analysis

Thermogravimetric curves were recorded on a Cahn 2000 electrobalance by heating from 298 to 1073 K at 10 K min^{-1} in a nitrogen atmosphere.

Chemical and Textural Properties

The specific surface areas of the solids were determined by using the BET method on a Micromeritics ASAP 2000 analyzer.

Basic sites were quantified from the retention isotherms for phenol ($pK_a = 9.9$), dissolved in cyclohexane. To this end, we used a measuring method that had previously proved highly effective for measuring the acidity and basicity of other porous solids. The amount of titrant retained by the solid was measured spectrophotometrically ($\lambda_{max} =$ 271.6 nm). By using the Langmuir equation, the amount of titrant adsorbed in monolayer form, X_m, was obtained as a measure of the concentration of basic sites (26).

NMR Spectroscopy

^1H and ^{71}Ga MAS NMR spectra were obtained at 400.13 and 121.98 MHz, respectively, on a Bruker ACP-400 spectrometer under an external magnetic field for 9.4 T. All measurements were made at room temperature following evacuation of the sample at 3 μm of Hg at 120°C for 3 h. The samples, containing in zirconia rotors, were spun at the magic angle (54°44′ relative to the external magnetic field) at 5 kHz. ^1H spectra were recorded after applying an excitation pulse of $\pi/2$ (5 μs) with a 2 s interval between successive accumulations to avoid saturation effects. ^{71}Ga spectra were recorded for an excitation pulse of $\pi/4$ (2 μs) and an accumulation interval of 3 s. Tetramethylsilane (TMS) and $Ga(H_2O)_6^{3+}$ (27) were used as external standards for the proton and gallium, respectively. The number of accumulations for the proton and gallium spectra were 200 and 6000, respectively.

RESULTS AND DISCUSSION

The elemental analysis of the Mg/Ga LDH following ion exchange with carbonate and drying in a stove at 393 K for 4 h gave the following formula for an Mg^{2+}/Ga^{3+} ratio of 2.50: $[Mg_{0.714}Ga_{0.286}(OH)_2][CO_3]_{0.143} \cdot mH_2O$.

The XRD analysis of the solid showed the synthetic LDH to be highly crystalline in both its original form (HT-1) and after ion exchange (HT-2). Figure 1 shows the X-ray diffractograms for the samples stored at 393 K. They are typical of solids with stacked layers and analogous to those previously

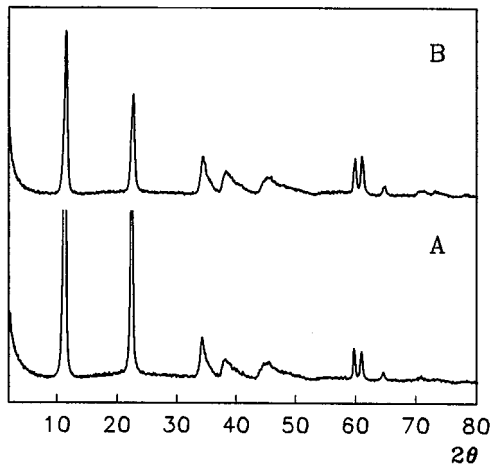

FIG. 1. XRD patterns for (A) HT-1 and (B) HT-2.

obtained by Reichle *et al.* (19) for Mg/Al LDH. From the position of the strongest lines, of crystallographic indices (003), the lattice distance d_{003} was obtained; this in turn was used to calculate the lattice parameter c. Such a distance was decreased by the ion exchange (see Table 1 for sample HT-1 and HT-2) as a result of the increased attraction between brucite-like layers and CO_3^{2-} ions, of greater charge than NO_3^- ions. Also, lattice parameter a, determined from the (001) diffraction, was decreased, consistent with an increase in the average particle size. A comparison of the values for the lattice parameters with reported values for Mg/Al LDHs with an Mg/Al ratio of 2.5 reveals that the chief effect of replacing aluminium with gallium in the LDH structure is an increase in the interlayer distance as a result of the higher atomic radius of gallium. Thus, Mg/Al LDHs with an Mg/Al ratio of 2.5 were found to have an a value of 3.046 (1) and 3.052 Å (20), and their parameter c to be 23.06 (1) and 23.08 Å (20).

Structural changes produced by calcination in the LDH sample that was subjected to carbonate exchange were monitored from XRD patterns (Fig. 2). Heating of sample HT-2 at 523 K (HT-3, Fig. 2A) caused no alteration or significant change in the lattice parameters (see Table 1). On the other hand, a calcination temperature of 823 K destroyed the LDH structure and led to the formation of a

TABLE 1
Lattice Parameters for Synthesized LDHs

Sample	T (K)[a]	d_{003} (Å)	a (Å)	c (Å)
HT-1	RT[b]	7.99	3.25	23.91
HT-2	RT[b]	7.93	3.10	23.79
HT-3	523	7.92	3.12	23.74

[a] Temperature of termic treatment.
[b] Room temperature.

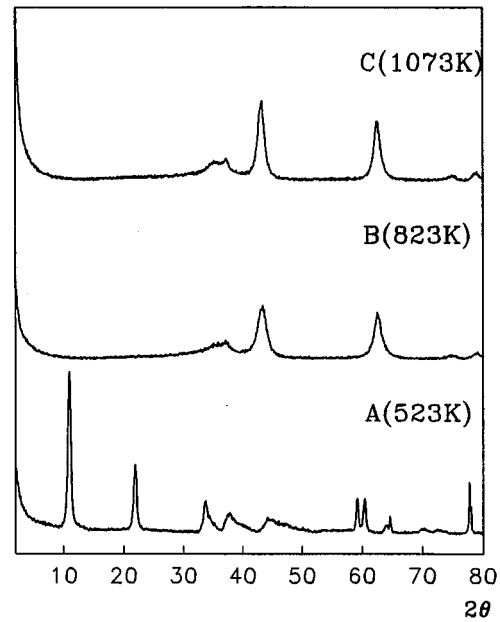

FIG. 2. XRD patterns for (A) HT-3, (B) HT-4, and (C) HT-5.

periclase magnesium oxide phase together with amorphous gallium oxide (Fig. 2B). Finally, raising the temperature from 823 to 1073 K caused no additional structural change in the phase formed at the former temperature (Fig. 2C).

Figure 3A shows the DRIFT spectrum for sample HT-2. As can be seen, it includes a strong band between 3800 and 2700 cm^{-1} that comprises the twisting vibrations of physisorbed water (28), vibrations of structural OH^- groups (29), characteristic valent vibrations of $OH \cdots OH$, and/or characteristic stretching vibrations of Mg^{2+}–OH^- bonds in Mg/Ga hydroxycarbonates similar to those for Mg/Al hydroxycarbonates (28–31). The band corresponding to the vibration mode δ_{HOH} appears at 1643 cm^{-1}. The sharp band at 1385 cm^{-1} corresponds to mode ν_3 of interlayer carbonate. This vibrational mode might also correspond to ν_3 for the nitrate ion—this, however, was confirmed to be absent from the LDH structure after the carbonate exchange. The restricted symmetry in the interlayer space activates mode ν_1 for carbonate, which occurs as a weak shoulder at 1049 cm^{-1}, consistent with previous results for other LDHs (32). There is no sign of bicarbonate species in the FTIR spectrum, however.

Figures 3B and 3C show the diffuse reflectance FTIR spectra for the Mg/Ga LDH samples calcined at 823 (HT-4) and 1073 K (HT-5), respectively. Both exhibit significant changes relative to the spectrum for the previous sample (Fig. 3A). The bands between 450 and 650 cm^{-1} correspond to characteristic vibrations of MgO and Ga_2O_3 (33, 34). The broad band centered at 1400 cm^{-1} is characteristic of O–C–O vibrations in adsorbed (not interlayer) carbonate groups on the surface of the oxide system formed (34, 35), as

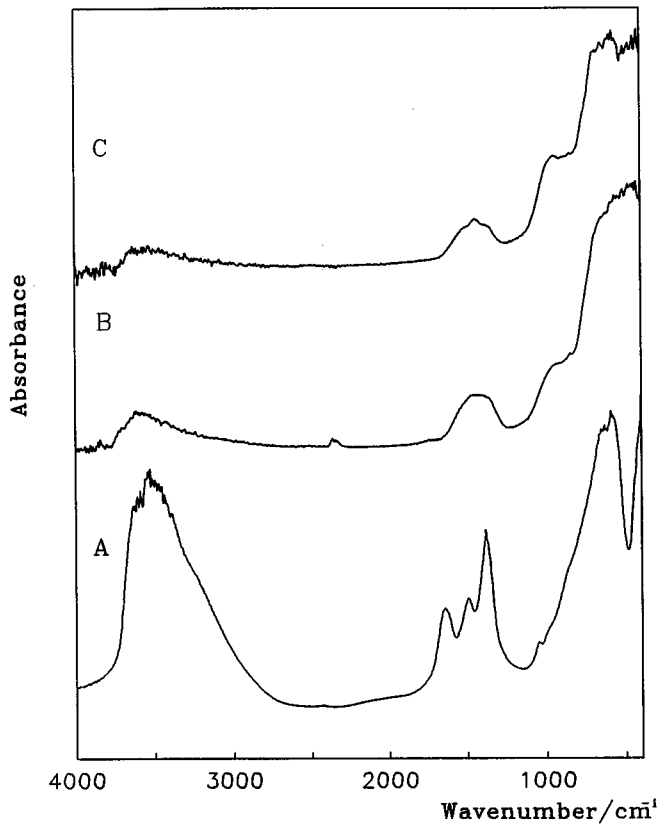

FIG. 3. DRIFT spectra for (A) HT-2, (B) HT-4, and (C) HT-5.

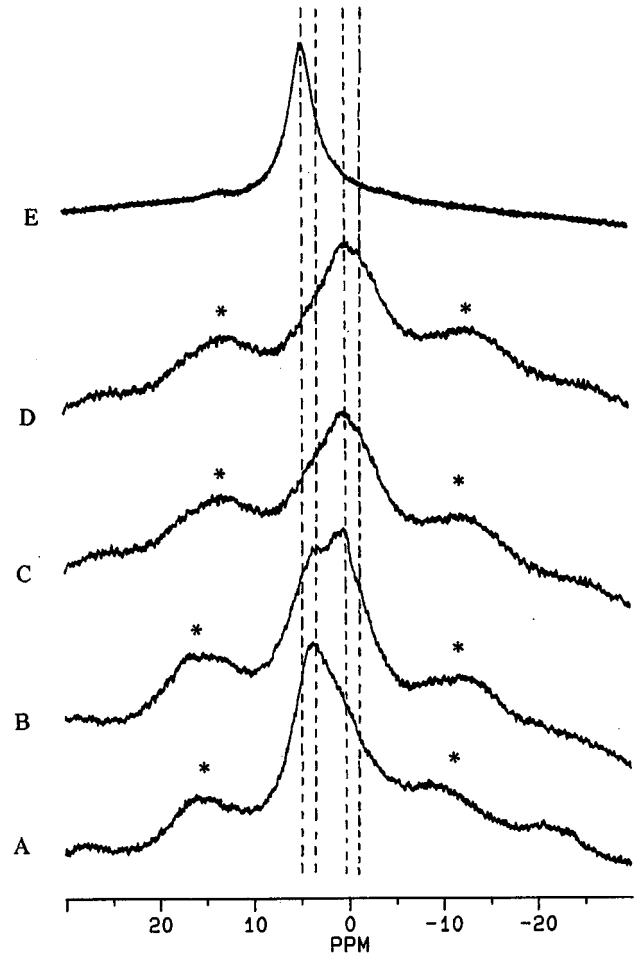

FIG. 4. ^{1}H MAS NMR spectra for (A) HT-2, (B) HT-3, (C) HT-4, (D) HT-5, and (E) MgO. Asterisks denote spinning side bands.

well as of carbonate and water reversibly adsorbed on the oxide surfaces (34–37). When the carbonate is massic or part of some other mixed structure (e.g., residual carbonate remaining after the synthesis of a magnesium orthophosphate) it is assigned a slightly higher frequency than interlayer carbonate, viz. 1432 cm^{-1} (38, 39). One other weak band is observed in the 3800–3100 cm^{-1} region due to the valent vibrations of $OH \cdots OH_2$ (28) and $H_2O \cdots OH_2$ (29). A high-temperature treatment therefore eliminates all these bands and that at 1400 cm^{-1}. Based on these results, the loss of water and CO_2 from these solids is quite apparent.

The TGA curves for sample 2 exhibit two stages spanning the ranges 423–490 and 563–693 K, respectively, which involve an overall weight loss of 41.5%. The first such loss (11.4%) can be ascribed to the release of weakly adsorbed interlayer water; the second (30.1%) is associated with the removal of water molecules from the brucite-like structure and of CO_2 from interlayer carbonate as the layered structure is destroyed.

Figure 4 shows the ^{1}H MAS NMR spectra for sample HT-2 (Fig. 4A), as well as those for the solids resulting from the thermal treatments at 523 K (HT-3, Fig. 4B), 823 K (HT-4, Fig. 4C), and 1073 K (HT-5, Fig. 4D). By way of comparison, Fig. 4E shows the spectrum for MgO calcined at 773 K. The spectrum for Mg/Ga LDH subjected to no thermal treatment (Fig. 4A) exhibits a signal at 4.1 ppm that can be ascribed to structural OH groups in the LDH and to physisorbed water. The asymmetry of the signal suggests the presence of another component overlapped with the previous one, which, by comparison with the spectrum for Mg/Ga LDH heated at 523 K (Fig. 4B), can be ascribed to Ga–OH groups ($\delta = 0.4$ ppm). In the spectrum, the intensity of the signal at 4.1 ppm appears to have been decreased by the dehydroxylation caused by the thermal treatment. It includes a signal at $\delta = -1.1$ ppm which, by analogy with reported results for aluminas (40, 41), can be assigned to OH groups where the proton is strongly shielded (e.g., basic octahedral Ga–OH groups). When the temperature is raised up to 823 or 1073 K (Figs. 4C and 4D, respectively), the intensity of the signals decreases owing to the loss of both interlayer OH groups and physisorbed water (the band at 4.1 ppm disappears), which leads to the destruction of the layered structure and the formation of the MgO and Ga_2O_3 phases. Thus, these spectra exhibit two distinct signals at

−1.1 and 0.4 ppm. Mastikhin (40, 41) assigned a signal at 0.33 ppm for aluminas to "basic" octahedral Al–OH groups and another at 2.55 ppm to "more acidic" Al–OH groups. By analogy with these results, the signal at −1.1 ppm can be ascribed to "basic" octahedral Ga–OH groups and that at 0.4 ppm to "more acidic" Ga–OH groups. On the other hand, by comparison with the ^{1}H spectrum for MgO the asymmetry of these signals suggests the presence of Mg–OH groups, although in much smaller numbers than Ga–OH groups.

Figure 5 shows the ^{71}Ga MAS NMR spectra for sample HT-2 (Fig. 5A) and those for the solids obtained on calcination at 523 K (Fig. 5B), 823 K (Fig. 5C), and 1073 K (Fig. 5D). The chemical shifts of the solids were subjected to no second-order quadrupole correction. A linear correlation was recently established between ^{27}Al and ^{71}Ga NMR chemical shifts in isostructural Al and Ga compounds possessing oxygen only in the first aluminium or gallium coordination sphere (42). Based on this correlation, and on available knowledge on the ^{27}Al NMR, chemical shifts for aluminium in aluminophosphates, approximate ^{71}Ga NMR chemical shift ranges for gallium in gallophosphates in terms of coordination number were predicted. The shifts for tetrahedrally coordinated gallium in galloaluminate-based MCM-41 molecular sieves and zeolites range from 139 to 156 (43–45). The shifts for octahedrally coordinated Ga in Mg/Ga LDH obtained by us from ^{71}Ga MAS NMR spectra (approximately from −14 to −21 ppm) and those for tetrahedrally coordinated Ga (58–59 ppm) can be correlated with those reported for Mg/Al LDHs with M^{2+}/M^{3+} ratios similar to those in our Mg/Ga LDH by using the linear relation reported by Bradley *et al.* (42).

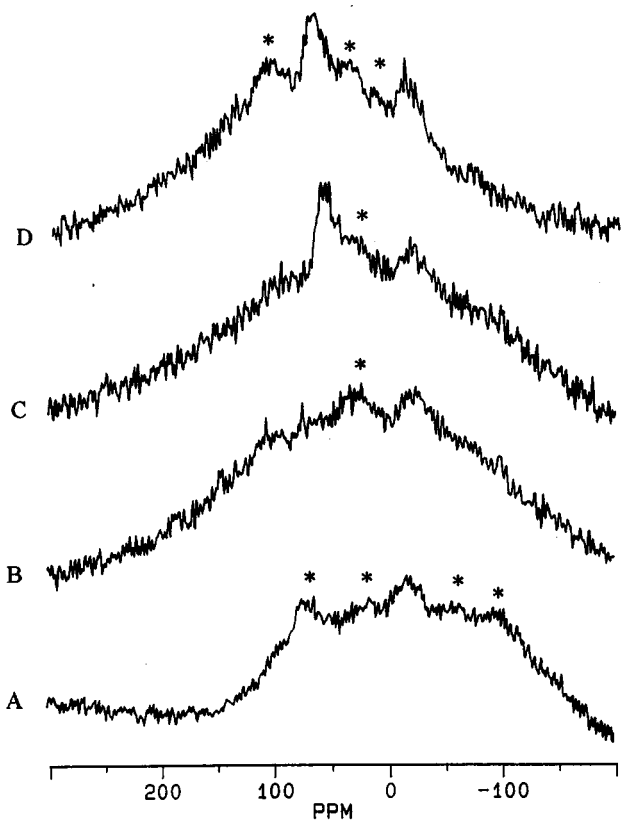

FIG. 5. ^{71}Ga MAS NMR spectra for (A) HT-2, (B) HT-3, (C) HT-4, and (D) HT-5. Asterisks denote spinning side bands.

Thus, solid HT-2 exhibited a typical signal for octahedral Ga at about −14 ppm (Fig. 5A), even though the quality of the spectrum was not too good. The broad band on which this signal was superimposed suggests that this gallium is in a distorted, low-symmetry environment. Calcining this material at 523 K (Fig. 5B) resulted in a upfield shift in the signal for octahedral Ga to −19 ppm; no signal for tetrahedrally coordinated Ga was observed because the material was still preserved its layered structure, as confirmed by the XRD study (Fig. 2A). On the other hand, calcination at 823 or 1073 K (Figs. 5C and 5D) revealed the presence of octahedral Ga (signal at ca. −20 ppm) and of tetrahedrally coordinated Ga (signal at 58–59 ppm). Based on previous results for Mg/Al LDHs (46–48), this new tetrahedral Ga probably arises from breakage of LDH layers and transformation of amorphous Ga_2O_3, which contains both coordination forms. These results are quite consistent with our ^{1}H MAS NMR results: OH groups are bonded to octahedrally coordinated gallium, which, as noted earlier, is present at calcination temperatures as high as 1073 K.

Table 2 gives the specific surface areas (S_{BET}) for the different samples and MgO and Ga_2O_3. As can be seen, the surface area increased with calcination of the sample at 823 K as a result of the removal of H_2O and CO_2 molecules, which increased the material's porosity and hence its area. A further increase in the calcination temperature to 1073 K diminished the specific surface area as the likely result of particle sintering. This was confirmed by X-ray diffractograms, which exhibited sharp peaks for the sample calcined thermally at 1073 K (Figs. 2B and 2C), thus suggesting

TABLE 2
Specific Surface Areas and Base Site Densities for Synthesized Mg/Ga LDHs and the Products of Calcination

Sample	T (K)[a]	S_{BET} (m^2/g)	X_m[c] (μmol/g)
HT-2	RT[b]	34.0	—
HT-3	523	18.1	133.7
HT-4	823	133.0	83.5
HT-5	1073	111.1	84.1
MgO	773	241.3	254.0
Ga_2O_3	773	6.1	35.1

[a] Temperature of termic treatment.
[b] Room temperature.
[c] Basicity.

improved crystallinity. These results are consistent with those reported for other LDHs (2, 48), even though they are highly influenced by the synthetic method used to prepare the LDH. However, a comparison of our results with those for Mg/Al LDHs with metal ratios of 2–4 reveals that the latter behave similarly toward calcination. The specific surface area of the untreated LDH is quite small and peaks at 723–823 K; above 823 K, it starts to decrease (2).

The basicity of the solids against phenol is given in Table 2. Before any CO_2 and H_2O are lost, the solid exhibits a strongly basic character that diminishes as the calcination temperature is raised. The basicity of the oxide mixture obtained on calcination is independent of the final calcination temperature. A comparison of this oxide mixture with its pure components (Table 2) reveals that the basic character of the mixture lies in between that of commercially available magnesium oxide and gallium oxide. However, as derived from the spectroscopic data, the mixture obtained by calcining the starting Mg/Ga LDH is not a simple mechanical mixture, but rather possesses peculiar structure and properties.

ACKNOWLEDGMENTS

The authors express their gratitude to Spanish DGICyT for financial support awarded for the realization of this work as part of Project PB92-0816, and to the staff of the Nuclear Magnetic Resonance Service of the University of Córdoba for their invaluable assistance in recording the NMR spectra.

REFERENCES

1. D. Tichit, M. H. Lhouty, A. Guida, B. H. Chiche, F. Figueras, A. Auroux, D. Bartalini, and E. Garrone, *J. Catal.* **151,** 50 (1995).
2. A. Corma, V. Fornés, and F. Rey, *J. Catal.* **148,** 205 (1994).
3. A. Corma, S. Iborra, J. Primo, and F. Rey, *J. Catal.* **114,** 215 (1994).
4. S. Vela and C. S. Swany, *Appl. Catal.* **119,** 241 (1994).
5. M. J. Climent, A. Corma, S. Iborra, and J. Primo, *J. Catal.* **151,** 60 (1995).
6. D. E. Laycock, R. J. Collacott, D. A. Skelton, and M. F. Tchir, *J. Catal.* **130,** 354 (1991).
7. T. Nakatsuka, H. Kawasaki, S. Yamashita, and S. Kohjiya, *Bull. Chem. Soc. Jpn.* **52,** 2449 (1979).
8. G. Fornasari, S. Gusi, F. Trifirò, and A. Vaccari, *Ind. Eng. Chem. Res.* **29,** 1500 (1987).
9. P. Courty and C. Marcilly, *Stud. Surf. Sci. Catal.* **16,** 485 (1983).
10. P. Courty, D. Durand, E. Freund, and A. Sugier, *J. Mol. Catal.* **17,** 241 (1982).
11. A. Sugier and E. Freund, U.S. Patent 4122100 (1978).
12. E. C. Kruissink, L. L. Van Reijen, and J. R. H. Ross, *J. Chem. Soc., Faraday Trans. I* **77,** 649 (1981).
13. L. E. Alzamora, J. R. H. Ross, E. C. Kruissink, and L. L. Van Reijen, *J. Chem. Soc., Faraday Trans. I* **77,** 665 (1981).
14. J. R. Rostrup-Nielsen, "Steam Reforming Catalysts," Teknisk Forlag, Copenhagen, 1975.
15. L. M. Parker, N. B. Mileston, and R. H. Newman, *Ind. Eng. Chem. Res.* **34,** 1196 (1995).
16. T. Sato, T. Wakabayashi, and M. Simada, *Ind. Eng. Chem. Prod. Res. Dev.* **25,** 89 (1986).
17. M. Jakupca and P. K. Dutta, *Chem. Mater.* **7,** 989 (1995).
18. I. C. Chisem and W. Jones, *J. Mater. Chem.* **4,** 1737 (1994).
19. W. T. Reichle, S. Y. Kang, and D. S. Everhardt, *J. Catal.* **101,** 352 (1986).
20. S. Miyata, *Clays Clay Miner.* **23,** 369 (1975).
21. S. Miyata, T. Kumura H. Hattori, and K. Tanabe, *Nippon Kagaku Zasshi* **92,** 514 (1971).
22. F. Cavani, F. Trifirò, and A. Vaccari, *Catal. Today* **11,** 173 (1991).
23. K. Fuda, N. Kudo, S. Kawai, and T. Matsunaga, *Chem. Lett.* 777 (1993).
24. D. Massiot, I. Farnan, N. Gautier, D. Trumeau, A. Trokiner, and J. P. Coutures, *Solid State NMR* **4,** 241 (1995).
25. S. M. Bradley, R. F. Howe, and J. V. Hanna, *Solid State NMR* **2,** 37 (1993).
26. M. A. Aramendía, V. Borau, C. Jiménez, J. M. Marinas, and F. Rodero, *Colloids Surf.* **12,** 227 (1984).
27. J. W. Akkitt, *Ann. Rep. NMR Spectrosc. A* **5,** 465 (1972).
28. G. Allegra and G. Ronca, *Acta Crystallogr. A* **34,** 1006 (1978).
29. D. Roy, R. Roy, and E. Osborn, *Am. J. Sci.* **251,** 337 (1953).
30. F. Mumpton, H. Jaffe, and C. Thompson, *Amer. Mineral.* **50,** 1893 (1965).
31. R. Allmann, *Chimia.* **24,** 99 (1970).
32. M. J. Hernández-Moreno, M. A. Ulibarri, J. L. Rendón, and S. J. Serna, *Phys. Chem. Mater.* **12,** 34 (1985).
33. L. Mirkin, "Rentgenostructurnii Analiz-Inducirovanie Poroshkovih Rentgenogramm," Nakua, Moskow, 1981.
34. H. Miyata, W. Wakamiya, and I. Kibokawa, *J. Catal.* **34,** 117 (1974).
35. J. Lercher, C. Colombier, H. Vinec, and H. Noller, *in* "Catalysis by Acids and Bases" (B. Imelik, C. Maccache, G. Cardurier, Y. Ben Taarit, and J. C. Vedrine, Eds.), p. 25. Elsevier, Amsterdam, 1985.
36. P. Tarte, "Proceedings of the International Conference on Physics of Non-Crystalline Solids," p. 549, 1965.
37. Y. Takita and J. Lunsford, *J. Phys. Chem.* **83,** 683 (1979).
38. M. A. Aramendía, V. Borau, C. Jiménez, J. M. Marinas, F. J. Romero, J. Navio, and J. Barrios, *J. Catal.* **97,** 157 (1995).
39. K. Nakamoto, "Infrared and Raman Spectra of Inorganic Compounds," 4th ed., p. 139. Wiley, New York, 1986.
40. V. M. Mastikhin, *Colloids Surf. A Physicochem. Eng. Aspects* **78,** 143 (1993).
41. V. M. Mastikhin, I. L. Mudrakovskii, and A. V. Nosov, *Prog. NMR Spectrosc.* **23,** 259 (1991).
42. S. M. Bradley, R. D. Howe, and R. A. Kydd, *Magn. Reson. Chem.* **31,** 883 (1993).
43. V. R. Choudhary, A. K. Kinage, C. Siradinaraya, P. Devadas, S. D. Sandre, and M. Guisnet, *J. Catal.* **158,** 34 (1996).
44. C.-F. Cheng and J. Klinowski, *J. Chem. Soc., Faraday Trans.* **92,** 289 (1996).
45. C.-F. Cheng, H. He, W. Zhou, J. Klinowski, J. A. Souza Goncalves, and L. F. Gladden, *J. Phys. Chem.* **100,** 390 (1996).
46. F. Rey, V. Fornés, and J. M. Rojo, *J. Chem. Soc., Faraday Trans.* **88,** 2233 (1992).
47. K. J. D. Mackenzie, R. H. Meinhold, B. L. Sherriff, and Z. Xu, *J. Mater. Chem.* **3,** 1263 (1993).
48. O. Clause, B. Rebours, E. Merlen, F. Trifirò, and A. Vaccari, *J. Catal.* **123,** 231 (1992).